Tip-Enhanced Raman Spectroscopy: Near-Fields Acting on a Few Molecules

Bruno Pettinger, Philip Schambach, Carlos J. Villagómez, and Nicola Scott

Department of Physical Chemistry, Fritz Haber Institute of the Max Planck Society, 14196 Berlin, Germany; email: pettinger@fhi-berlin.mpg.de

Annu. Rev. Phys. Chem. 2012. 63:379–99

First published online as a Review in Advance on January 20, 2012

The *Annual Review of Physical Chemistry* is online at physchem.annualreviews.org

This article's doi: 10.1146/annurev-physchem-032511-143807

0066-426X/12/0505-0379$20.00

Keywords

field enhancement, surface plasmons, TERS, beyond diffraction limitation, single molecule

Abstract

Tip-enhanced Raman spectroscopy (TERS) is a very powerful variant of surface-enhanced Raman spectroscopy (SERS). In a sense, TERS overcomes most of the drawbacks of SERS but keeps its advantages, such as its high sensitivity. TERS offers the additional advantages of high spatial resolution, much beyond the Abbe limit, and the possibility to correlate TER and other scanning probe microscope images, i.e., to correlate topographic and chemical data. TERS finds application in a number of fields, such as surface science, material science, and biology. Single-molecule TERS has been observed even for TERS enhancements of "only" 10^6–10^7. In this review, TERS enhancements are discussed in some detail, including a condensed overview of measured contrasts and estimated total enhancements. Finally, recent developments for TERS under ultrahigh vacuum conditions are presented, including TERS on a C_{60} island with a diameter of a few tens of nanometers, deposited on a smooth Au(111) surface.

1. INTRODUCTION

Tip-enhanced Raman spectroscopy (TERS): a powerful variant of surface-enhanced Raman spectroscopy (SERS)

Surface-enhanced Raman spectroscopy (SERS): an enhanced Raman process occurring for molecules adsorbed at specifically structured surfaces of coinage metals

Raman spectroscopy: the scientific field of inelastically light scattering by matter (gasses, liquids, solids)

UHV: ultrahigh vacuum

EM: electromagnetic

Chemical enhancement: refers to all local enhancement mechanisms related to the creation or changes of molecular orbitals facilitating (pre)resonant Raman processes

Charge transfer enhancement: the inelastic scattering of excited metal electrons by an adsorbate, a variant of chemical enhancement

Surface plasmons: excitations of collective electron oscillations in metal surfaces or in nanoparticles made of coinage metals

Tip-enhanced Raman spectroscopy (TERS) (1–4) is a very powerful variant of surface-enhanced Raman spectroscopy (SERS). SERS, detected in the mid 1970s, has substantial drawbacks; for example, intense SERS occurs only for roughened substrates made of coinage metals or for clusters of nanoparticles, again made of coinage metals (5).[1] In contrast to SERS, TERS operates on all adsorbate/substrate configurations, where the substrate may be rough or smooth (7), or even single crystalline (8), and can be either a metal (4), a semiconductor (9, 10), or an isolator (1) and where the adsorbate may or may not be in optical resonance with the exciting laser line (11). However, only a limited number of such systems have been investigated to date, but all results continue to indicate the very promising nature of TERS. Furthermore, due to the strong localization and height of the optical near-fields underneath the tip, TERS delivers with very high sensitivity, via Raman spectroscopy, chemical information on the nanometer scale; some reports already indicate that the single molecule detection level has been reached (12).

In this review, we begin with a short overview of SERS, focusing on its strengths and drawbacks, followed by an overview of TERS and its recent developments. We first address early TERS experiments, followed by a discussion on contrast and underlying enhancement and a specific, condensed overview of this topic. In the few-molecule TERS section, we address the requirements of few- or single-molecule TERS and present two examples in which UHV-TERS is employed.

2. SURFACE-ENHANCED RAMAN SPECTROSCOPY

Richard P. Van Duyne and coworkers (13) were the first to notice a very strong surface enhancement for Raman scattering performed on pyridine molecules adsorbed at silver (Ag) electrodes. Van Duyne repeated and extended the striking experiments of McQuillan et al. (14) and Fleischmann et al. (15), who observed strong Raman scattering for pyridine adsorbed at Ag electrodes that had been electrochemically roughened. Fleischmann et al. (14, 15) attributed the observability of a Raman signal to a substantial increase of adsorption sites for roughened Ag electrodes. Van Duyne, however, estimated an approximately 10^5–10^6-fold increase of the Raman signal in comparison to the signal expected for a monolayer of pyridine adsorbed on a smooth Ag surface. Obviously, this almost millionfold increase of the Raman intensity upon roughening cannot be attributed to an increase in adsorption sites. Instead, the increase had to be attributed to a surface-enhancement process of an as yet unknown nature.[2]

Today's consensus is that SERS involves two enhancement mechanisms, so-called chemical and electromagnetic (EM) enhancements, often occurring at quite different strengths.[3] Chemical enhancement accounts for the chemical specificity of SERS (not all molecules will be enhanced equally),[4] whereas EM enhancement is thought to operate on all adsorbates equally, with the exception of some polarization and molecular orientation effects that influence the (relative) Raman intensities to some extent. This latter enhancement mechanism is associated with the excitation of surface plasmons and the strength of their EM fields near the surface. These fields can be significantly larger than the incident fields. Together, chemical and EM enhancement may lead to an overall average enhancement of approximately 10^6, as already reported by Van Duyne (13)

[1] Weak SERS for transition metal substrates was shown by Z.Q. Tian (6) in the late 1990s.

[2] A year later, Van Duyne et al. (16) presented an image field model that was soon disregarded in favor of surface plasmon-mediated enhancement (5).

[3] This concept of two cooperative surface enhancement mechanisms had already been proposed in the early 1980s (17–20).

[4] In the following, chemical enhancement will not be considered in more detail due to the specific theme of this review.

for pyridine on Ag electrodes. Surprisingly, findings in the late 1990s disclosed huge variations of surface enhancement along a rough surface or over colloidal systems (21–26). Obviously, within such structures, so-called hot spots occur that can provide extremely high enhancements locally. Theory and experiments indicate that a few hot spots may make up most of the enhanced Raman signal, in contrast to the vast majority of sites that do not contribute significantly. The hot spots were believed to be specific interstitial sites between colloidal clusters or structural elements of roughened surfaces, where the field enhancement becomes extremely large (27). As such sites are in a sense hidden, and thus not accessible for detailed investigation, their precise nature is not yet experimentally clarified.

Hot spots: spatially narrow regions of strongly enhanced electromagnetic fields occurring, e.g., in narrow gaps between nanoparticles

Electromagnetic enhancement: the enhancement of Raman scattering related to the enhanced near-field of excited (localized) surface plasmons

Theory has shown, however, that if a dimer of two suitable nanoparticles is illuminated, a strong enhancement of the EM field can occur in the narrow space between the two particles (28–31). Let us describe the field enhancement for the incident EM wave by a factor g_i, and the enhancement of the scattered field by g_{sc}. A hundredfold increase of the EM field relative to the incident one (i.e., $g_i = 100$) would result in a local 10,000-fold intensity ($I_{loc} = g_i^2 I_0$), and the total surface enhancement would rise to 10^8 locally, assuming the g^4 law to be valid.[5] Clear proof for the hot spot character of SERS originated from single-molecule SERS experiments, which could succeed only if a single molecule, located in the hot spot zone, were selectively exposed to a significant enhancement, whereas nearby molecules experienced only a minor enhancement. Kneipp et al. (33) and Nie & Emory (34) claimed enhancement factors of 10^{14} or higher (32–35). Although such large enhancement factors have recently been disregarded, the hot spot scenario remains valid. The maximal enhancement for SERS appears to be in the range of 10^{10}–10^{11} (36, 37).

In spite of the success of SERS, in terms of its outstanding sensitivity, conventional SERS has a number of drawbacks, such as the following:

1. The total degree of surface enhancement depends on the nature of the molecules.
2. SERS is mainly limited to substrates made of coinage metals such as copper, silver, and gold.
3. The hot spot scenario means that atypical/unknown sites for adsorption/chemisorption contribute the most to the surface enhancement; thus, SERS spectra may not be representative for the majority of sites.
4. EM and chemical enhancements can be inseparably intertwined.[6]

These drawbacks clearly indicate that SERS can not be used as routine spectroscopy in general.[7] In spite of SERS' success, the old dream to perform Raman spectroscopy at smooth or even single crystalline interfaces remained a dream for a long time. Of course, several attempts were made in that direction, but success was limited: On smooth or single crystalline surfaces, surface plasmons cannot be excited by direct illumination; thus, electromagnetic enhancement is basically absent, and only chemical enhancement can prevail, if this enhancement is possible at all (41–45).

The question arises: Is it possible to overcome the above-mentioned limitations of SERS? The answer comes primarily from the theoretical concept of enhanced near-fields: By the 1980s, a concept had already been proposed that would permit the creation of strongly enhanced EM

[5] For $g \approx g_{sc} \approx g_i$, the EM part of the enhancement is simplified to $F_{EM} = g_i^2 g_{sc}^2 \approx g^4$.

[6] Even if the chemical enhancement is weak (~10–100-fold), it may alter Raman frequencies, relative intensities, and if symmetry changes occur, may also cause the appearance or disappearance of (new) Raman bands.

[7] This is due to point 4, which does not hold for TERS. The many attempts to overcome this problem, e.g., to functionalize the surfaces (38–40), are based on a strategy being analogous to that of TERS: the target molecules are separated from the surfaces (in the case of TERS they are separated from the tip); then, only the EM enhancement is operating. Under such or analogous conditions, the prevailing electromagnetic enhancement mechanism acts equally on all molecules located in the field-enhancement zone and, then, SERS may become an analytical tool as well.

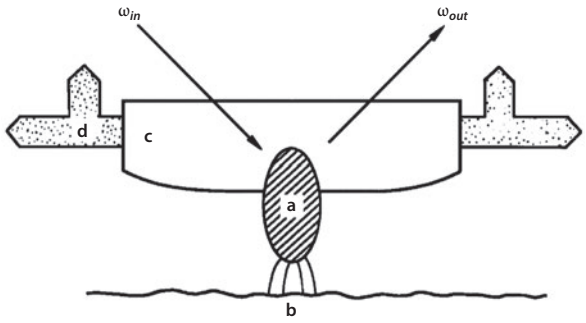

Figure 1

The optical probe particle (*a*) intercepts an incident laser beam, of frequency ω_{in}, and concentrates the field in a region adjacent to the sample surface (*b*). The Raman signal from the sample surface is reradiated into the scattered field at frequency ω_{out}. The surface is scanned by moving the optically transparent probe-tip holder (*c*) by piezoelectric translators (*d*). Reprinted with permission from Reference 50. Copyright 1985 Optical Society of America.

fields in the vicinity of a smooth surface by placing spheres or even a single sphere next to a flat metallic or semiconducting surface (46–49). Illumination from above should thereby create electromagnetic fields in the gap between the sphere and the flat surface that would be stronger than those on the sphere alone.

At approximately the same time, 1985, Wessel (50) proposed a similar but extended concept: combining the use of a single metal nanoparticle with a scanning tunneling microscope (STM) that could be rastered over a surface (**Figure 1**). The nanoparticle acts as an antenna for incident and reradiated fields. Wessel noted that his approach might be suitable for enhanced Raman, two-photon or second-harmonic spectroscopy, to detect even single molecules (50). Approximately 15 years later, Wessel's idea was realized by the Zenobi group (1), but using an atomic force microscope (AFM) and a cantilever tip covered with an approximately 50-nm-thick Ag film; the authors showed TERS for C_{60} and brilliant cresyl blue (BCB) molecules with a spatial resolution of <50 nm (1).

3. TIP-ENHANCED RAMAN SPECTROSCOPY

Scanning tunneling microscope (STM): the height of the tunneling current between tip and sample surface is used to record the sample's topography

Atomic force microscope (AFM): the force between tip and surface atoms is the sensor for recording the topography of a sample

BCB: brilliant cresyl blue

The scheme of TERS is straightforward. The crucial part is the combination of a scanning probe device with a Raman spectrograph, where the scanning probe device can be an AFM, a shear force microscope, or an STM. The experimental arrangement of the two parts permits illumination of tip and sample by an incident laser beam and recording of Raman scattering from the focal region. **Figure 2** illustrates this scheme, depicting the excitation of surface plasmons that produce enhanced near-fields in the vicinity of the tip apex. If the tip is located close to the sample, the enhanced near-fields cause an enhanced Raman scattering. In effect, the metalized tip acts as an optical antenna that enhances both the incident and the emitted fields. Suitable tips are quite important: either an AFM tip covered with a thin layer of Ag or Au or an STM tip, usually made of a thin Ag or Au wire having a sharpened end. The shape and curvature of the tip end determines both the enhancement and the spatial resolution of TERS.

It was evident right from the start that TERS not only overcomes the above described limitations of SERS but also offers the possibility of moving toward single molecule detection, as predicted by Wessel (50). In fact, TERS—representing a single hot spot—exhibits an extreme sensitivity as well as a high spatial resolution, down to a few nanometers, thus permitting the

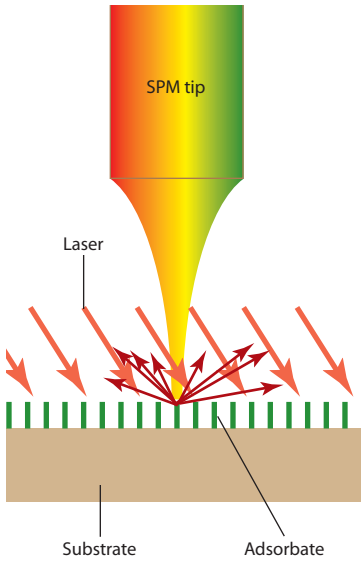

Figure 2

Tip-enhanced Raman spectroscopy. A laser light is focused on the scanning probe microscope (SPM) tip and sample. The minimum size of the focus is $\sim\lambda/2$. The near-field created in the vicinity of the tip causes the enhanced Raman scattering from a few molecules underneath the tip. The diameter of the near-field scattering zone is $\sim R_{tip}/2$, where R_{tip} is the curvature of the tip end.

correlation of scanning probe microscope (SPM) images with TER images i.e., of topographic with chemical data. This advantage of TERS led to its widespread application in the fields of biology (51–56) and physical chemistry, including surface science and materials science (9, 57–65).

3.1. Early TERS Experiments

In the first four papers reporting on TERS, all four groups used a similar inverted microscope approach; three employed an AFM or shear force technique, the fourth an STM.

The first published paper on TERS was that of Stöckle et al. (1), who studied C_{60} molecules and BCB molecules deposited as a thin layer on a glass support. The case of BCB is reproduced in **Figure 3** showing two experimental conditions (insets) for the two Raman spectra A and B. In the first experiment (inset a), the glass support with the thin dye layer is illuminated via an inverted microscope (not shown), whereas the silverized AFM tip is kept in a retracted position. Raman scattering was recorded from dye molecules in the focal regime and plotted as spectrum A. The AFM tip was then moved into contact with the dye layer and into the center of the focus (inset *b*). The illumination not only caused the Raman scattering, as seen before, but also an enhanced Raman scattering arising from the few molecules that were underneath the tip and exposed to the enhanced near-field of the illuminated tip. For the enhanced Raman process, the authors estimated an enhancement factor of approximately 10^4 (1).

Anderson (2) described a similar approach, using a Au-coated AFM cantilever tip to achieve enhanced Raman scattering from thin films of sulfur deposited on a quartz slide. A strong enhancement was seen only from the region of the illuminated tip (**Figure 4**, line A), whereas from a region 25 μm away, no Raman signal was detectable (**Figure 4**, line B). For the enhancement, Anderson gave a lower boundary of 10^4 (2).

Scanning probe microscope (SPM): a device that rasters a sharp tip over a surface to record the topography of the sample

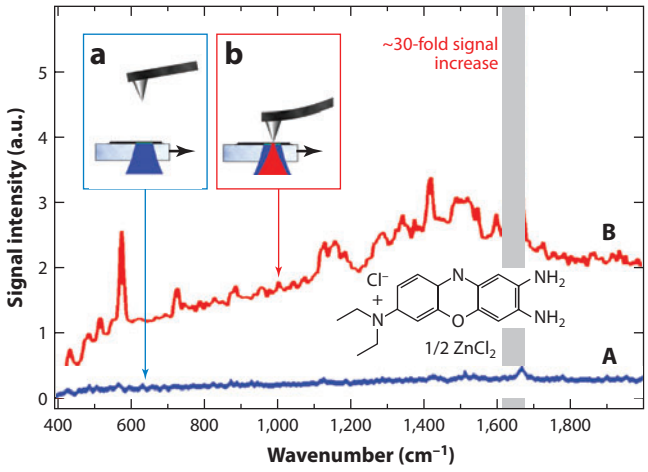

Figure 3

Tip-enhanced Raman spectra of brilliant cresyl blue dispersed on a glass support and measured with a silver-coated atomic force microscope probe. The two Raman spectra were measured with the tip retracted from the sample (*inset a*, *line A*) and the tip in contact with the sample (*inset b*, *line B*). Reprinted with permission from Reference 1. Copyright 2000 Elsevier Science B.V.

Rh6G: rhodamine 6g

Hayazawa et al. (3) reported near-field Raman spectroscopy on rhodamine 6g (Rh6G) deposited at a Ag-island film, also using the inverted microscope approach and an AFM with a silicon cantilever covered with a 40-nm-thick Ag film. The thickness of the Ag-island film was varied, and the highest SERS signals were achieved for a film thickness between 8 and 10 nm. The preparation of the Rh6G led to Rh6G crystals of approximately 50-nm diameter on the Ag surface (3). In **Figure 5**, the far- and near-field spectra of Rh6G on the Ag-island film are reproduced, where the so-called far-field spectrum obviously represents the sum of far-field plus surface-enhanced Raman spectra (the underlying Ag film was rough). Also noteworthy is the fact that Hayazawa

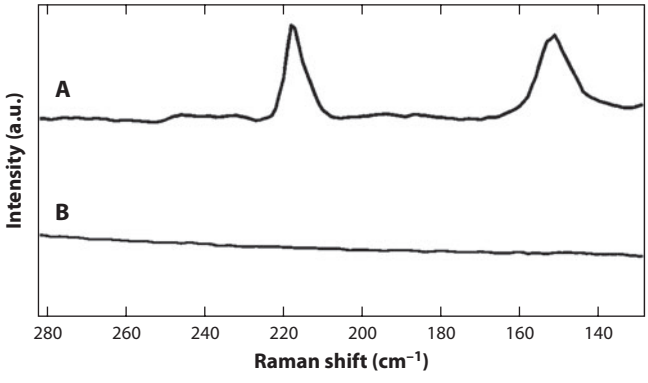

Figure 4

Raman spectrum demonstrating gold-coated atomic force microscope tip causing a local surface-enhanced Raman effect (*line A*) on a sulfur film. When the beam is focused away from the tip on the film, the Raman signal (*line B*) is undetectable using the same microprobe parameters. Reprinted with permission from Reference 2. Copyright 2000 American Institute of Physics.

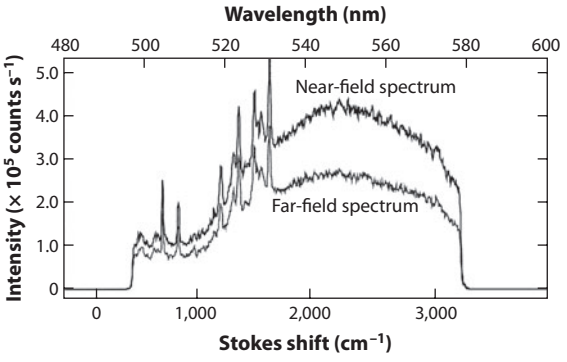

Figure 5

Near-field and far-field spectra. Raman spectra of Rh6G with a silver-coated atomic force microscope cantilever. Near-field (*black line*) and far-field (*gray line*) spectra correspond to the spectra with and without a cantilever at the tip-sample distance of 0 nm. The laser power is 0.5 mW and the exposure time is 5 s. Reprinted with permission from Reference 3. Copyright 2000 by Elsevier Science B.V.

et al. (3) illuminated the sample prior to the experiment with an argon ion laser line of 488 nm, in order "to minimize photobleaching effects." For these conditions, the authors estimated a 40-fold enhancement for TERS (3). However, they did not address the fact that observed SERS occurs in numerous so-called hot spots located anywhere in the focal area, but most likely not near or underneath the tip. Nevertheless, this comparison reveals an interesting circumstance: The single hot spot made by the tip-sample configuration is nearly as efficient in enhanced Raman scattering as the sum of all near-field configurations producing the SERS signal!

The approach of the Pettinger group (4) is similar to that of the first three papers as the authors also use the inverted microscope approach, but it differs in both the scanning-probe microscopy and the tip and sample preparation: An STM is combined with a Raman microscope, the tip is a Ag wire with a sharp end, and the sample is a monolayer of BCB molecules adsorbed on a very thin, smooth Au film evaporated on a glass slide. This metal film is only 12 nm thick and thus permits the inverted microscope approach by transmission of incident photons toward the tip and of the scattered photons back to the microscope. **Figure 6** depicts this specific approach, whereas **Figure 7** reproduces two spectra, one for the tip in retracted position and another for the tip in tunneling position. Again, these two curves and the corresponding insets refer to so-called far- or near-field spectra, which we have already encountered in the papers of Stöckle et al. (1), Anderson (2), and Hayazawa et al. (3). Pettinger et al. (4) used a low incident laser power of 0.05 mW (633 nm) to prevent fast photobleaching and observed a contrast of 15, i.e., a 15-fold larger TERS intensity than resonance Raman scattering (RRS) intensity in the far-field spectrum.

3.2. On TERS Enhancements

To estimate the EM part of the enhancement in TERS, one needs the values of the following variables: (*a*) the intensity of the TERS peak (the near-field intensity produced by the molecules underneath the tip), (*b*) the far-field intensity, (*c*) the area and depth of the focus, and (*d*) the area and depth of the near-field contributing to TERS.

In general, the TERS enhancement reads as

$$F_{EM} = \left(\frac{I_{nf} + I_{ff}}{I_{ff}} - 1 \right) \frac{V_{ff}}{V_{nf}},$$

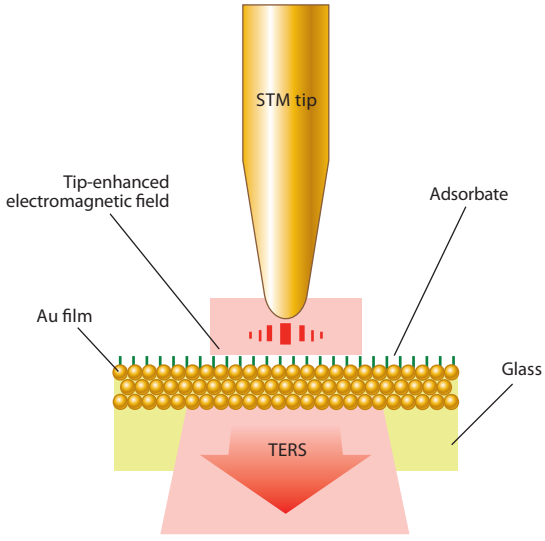

Figure 6

Tip-enhancement of Raman scattering. A scanning tunneling microscope (STM) is used; the substrate for a monolayer of brilliant cresyl blue molecules is a thin, smooth gold layer with an approximately 12 nm thickness deposited on a glass slide. For the inverted microscope approach, the thin metal layer is sufficiently transparent for the incident and emitted light; in addition, it is conductive enough to be employed within an STM. The tip is thin silver wire etched to a sharp point. Reprinted with permission from Reference 4. Copyright 2000 Electrochemical Society of Japan. Abbreviation: TERS, tip-enhanced Raman microscopy.

where the first term in the bracket represents the (measurable) contrast, and V_{ff} and V_{nf} are the volumes probed by the far- and near-fields, respectively.[8] When the tip is retracted from the sample, the measured Raman intensity is the so-called far-field intensity, I_{ff}, arising from the focal volume $V_f = R_{focus}^2 \pi\, h_{ff}$, where R_{focus} and h_{ff} are the focal radius and the effective depth of the focus (from which Raman scattering is collected), respectively. On the other hand, when the tip is in proximity to the sample, the measured Raman intensity includes both the far-field and the near-field contributions, denoted as $I_{nf} + I_{ff}$, where the near-field contributions arise from a rather small volume denoted as the TERS volume $(\frac{1}{2} R_{tip})^2 \pi\, h_{nf}$, with R_{tip} and h_{nf} being the tip radius and the effective height of the near-field, respectively. The factor 1/2 in front of R_{tip} is based on the approximation of $R_{TERS} \approx \frac{1}{2} R_{tip}$ (66). In many experimental cases, the angle of incidence of the beam is nonzero (relative to the normal of the surface); thus, an elliptic shape of the focus has to be accounted for, i.e., with the term cosα because the elliptic shape affects the focal intensity acting on the tip, but it does not affect the recorded far-field intensity, because the lower intensity is compensated for by the larger number of molecules in the elliptic-shaped focus.

For a sufficiently thin layer of adsorbed/deposited species, one can approximate $h_{ff} \sim h_{nf}$ and, thus, $V_{ff}/V_{nf} \approx R_{focus}^2/R_{TERS}^2$. The TERS enhancement is then

$$F_{EM} = \left(\frac{I_{nf} + I_{ff}}{I_{ff}} - 1 \right) \left(\frac{R_{focus}}{\frac{1}{2} R_{tip}} \right)^2 \cos\alpha.$$

[8]The underlying assumption is equal density and composition of matter in both cases.

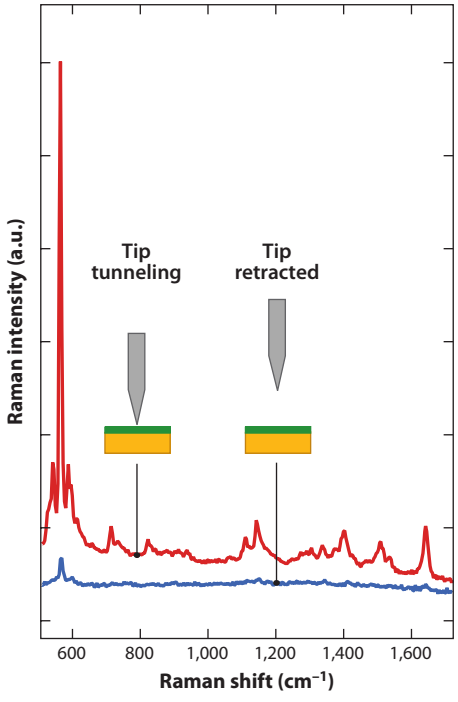

Figure 7

Comparison of a resonance Raman scattering spectrum with the tip-enhanced Raman spectrum of brilliant cresyl blue at a smooth, gold film. Coverage: 0.5 ML. Tunneling distance is 1 nm; retracted distance is 1,000 nm. Laser power at the sample is 0.05 mW at $\lambda = 633$ nm. Reprinted with permission from Reference 4. Copyright 2000 Electrochemical Society of Japan.

For example, assuming the parameter values reported in (8): For a contrast of $(I_{nf} + I_{ff})/I_{ff} = 10{,}000$, $R_{focus} = 1{,}000$ nm, $R_{tip} = 90$ nm, $\alpha = 60$, the second term becomes ~500, and the third is 1/2. In total, the overall TERS enhancement is then $F_{TERS} \sim 2.5 \times 10^6$.[9]

Steidtner & Pettinger (10) reported large contrasts for the case of a 1/2 monolayer of BCB adsorbed at a single crystalline surface of Au and platinum; for the former, with BCB at Au(111), the reported contrast is 3,900; the radii of the Au tip and the circular focus were 15 nm and 150 nm, respectively; due to the circular shape of the focus, $\cos\alpha = 1$; the overall TERS enhancement becomes $F_{TERS} \sim 1.6 \times 10^6$. If the tip radius were slightly larger, say 20 nm, the TERS enhancement would drop to $F_{TERS} \sim 8.8 \times 10^5$. For the second case, with BCB on Pt(111), the reported contrast is 1,390, and with the other terms as given above, the TERS enhancement is $F_{TERS} \sim 5.6 \times 10^5$.

Obviously, the estimation of the overall TERS enhancement also depends on parameters that are not precisely measurable, e.g., tip radius, focus radius, depth of focus and of near-field, and the angle of incidence. Even small errors of 20–50% in these values can result in substantial over- or underestimation of the TERS enhancement. Even greater error can arise from inhomogeneities in composition, density, and thickness of molecular films in the focal region; the far-field spectrum

[9]In the paper cited, the third term was not considered, and $R_{TERS} = R_{tip}$ was used instead of $R_{TERS} = \frac{1}{2} R_{tip}$; thus, the TERS enhancement was estimated at $F_{TERS} \sim 10^6$ (8).

represents an average over all local variations, whereas the near-field of the tip probes only a local element of the film.

S/N: signal-to-noise ratio

Figure 8 compares overall TERS enhancements together with the respective contrast reported in more than 20 papers.[10] To facilitate comparison, the data (bottom and top axis) are presented in a logarithmic scale, and the results are color coded for TERS, contrast, and whether an AFM or STM was used. As mentioned above, contrast is the ratio of the TERS intensity and the (unenhanced) Raman intensity (I_{TERS}/I_{Raman}). The reported contrast ranges between 1.5 and approximately 10,000, whereas the underlying total enhancement can be several orders of magnitude larger. This comparison shows that AFM-based TERS often yields rather low contrasts of <100, which usually means a TERS enhancement of $F_{TERS} \leq 10^4$. Exceptions are few and owe chiefly to a large V_{ff}/V_{nf}. On the other hand, high contrasts in the range of 1,000–10,000 are reported only for STM-based TERS. For V_{ff}/V_{nf} between 100–10,000, the underlying TERS enhancements span a range of $10^4 \sim 10^7$. For TERS enhancements of $\sim 10^6$ and higher, single-molecule measurements are feasible (12, 77).

3.3. Few-Molecule TERS

Large enhancement is a prerequisite for few- or single-molecule measurements and, consequently, a rather high stability of the sample/tip system is required under locally extreme incident intensities. For a better understanding of this issue, let us consider the case of an incident laser power of 1 mW and a sharp focus of approximately 300-nm diameter. For these parameters, the average intensity in the focal area becomes more than 1.4×10^6 W cm^{-2}. Reported TERS enhancements range from $\sim 10^3$ to 5×10^9. This corresponds to a local field enhancement of $g \sim 10$ to 250 and means the local intensity underneath the tip will rise by a factor of ~ 100 to 6×10^4; for the latter value, the local intensity may reach an incredible level of $>8 \times 10^{10}$ W cm^{-2}. Such high intensities provide continuously oscillating field strengths on the order of >2.8 V nm^{-1}! Can any molecule withstand such extreme field strengths?[11]

Evidently, extreme local intensities upon enhancement may become counterproductive; to account for associated disadvantages, one has to use a comparatively weak incident power of a few μW cm^{-2} (or a sufficiently large focus or short acquisition time) to avoid photobleaching, photochemical processes, sample heating, or desorption of molecules.

A clear signature of a high enhancement is a large contrast (TERS intensity/Raman intensity, or T/R), or if there is no Raman scattering detectable when the tip is retracted, a large TERS signal-to-noise ratio (S/N). Again, assuming adsorption of approximately a monolayer of large molecules such as dyes and a TERS radius of approximately 10 nm (the tip radius is then 20 nm), there are approximately 300 molecules located within the TERS radius, and they make up the total TERS signal. The height of this signal may already allow estimation of whether or not single-molecule detection is possible. In order to achieve single-molecule TERS, a significantly lower molecular coverage is required. Yet, a substantial T/R and S/N are needed, with values preferably >4, to facilitate the use of the fingerprint character of vibrational spectra. For practical reasons,

[10] From the literature, only papers that report contrast as well as the radii of tip and focus are considered; due to space constraints, only 21 papers could be considered; actually, among 220 TERS papers published to date, only 35 papers address the TERS enhancement and provide the required information.

[11] Enhancements of 10^{14} or larger are also in discussion; with the above parameters, the local intensity should reach levels of $>10^{13}$ W cm^{-2} (corresponding to field strengths of >25 V nm^{-1}!) continuously acting on the substrate, molecules, and tip. Recently, Etchegoin et al. (36) reported maximal SERS enhancements of approximately ten orders of magnitude; thus, for TERS, maximal enhancements by approximately nine orders of magnitude seem to be more realistic and are not even necessary for single-molecule detection (12, 77).

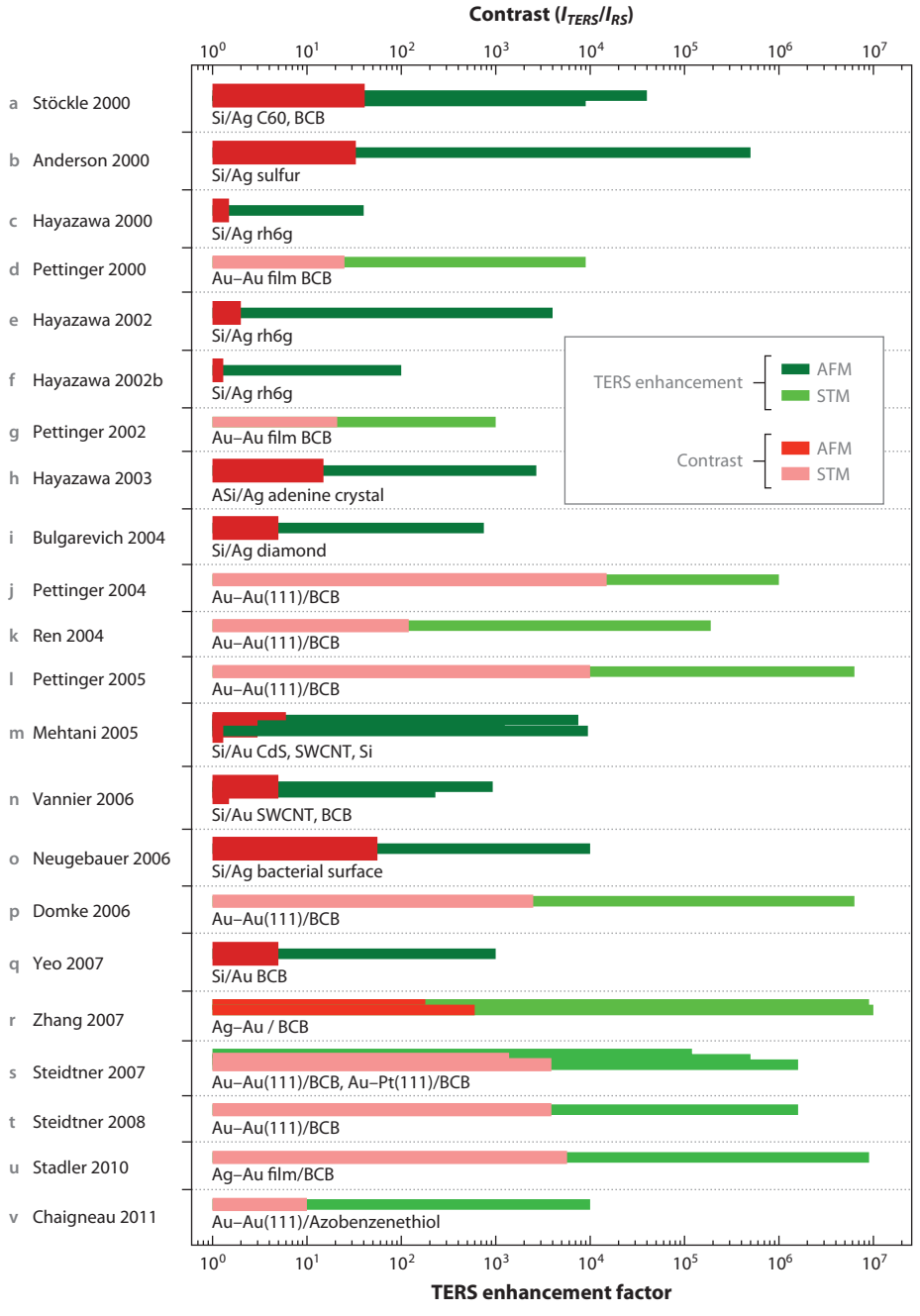

Figure 8

Reported overall tip-enhanced Raman spectroscopy (TERS) enhancements together with each contrast. For an easy comparison, the data are presented in a logarithmic scale (same scale for bottom and top axis), and the results are color coded for TERS, contrast, and whether an atomic force microscope (AFM) or scanning tunneling microscope (STM) was used.

there is an additional preference: the recording of TER spectra in (sub)second time intervals. Substantially extended acquisition times may not be a suitable solution to a low-signal problem, because, before the end of the measurement time, the single molecule (eventually observed by SPM imaging and then addressed by the illuminated tip) may disappear from the high-field zone by diffusion, desorption, photobleaching, photochemistry, and the like. Certainly, the above mentioned diffusion and desorption problems can be overcome by employing either low temperatures or by fixing the molecule to a specific adsorption site via strong chemical bonds.

The results published by Steidtner & Pettinger (10, 12) on the first extension of TERS to a UHV system using BCB as an adsorbate (**Figure 9**) are illustrative. This dye is in optical resonance with the exciting helium-neon laser line at 632.8 nm. Thus, upon excitation resonance, Raman processes take place, possibly in combination with tip-enhanced Raman processes. For the experiments described in (10), the preparation procedures led to a surface coverage of approximately 1/2 of a monolayer of BCB adsorbed at atomically flat Au(111) samples; here, Steidtner & Pettinger observed a strong band at 570 cm^{-1}, showing a TER peak intensity of approximately 7,800 cps, but for approximately 90 molecules located in the enhanced field zone. Thus, each BCB molecule

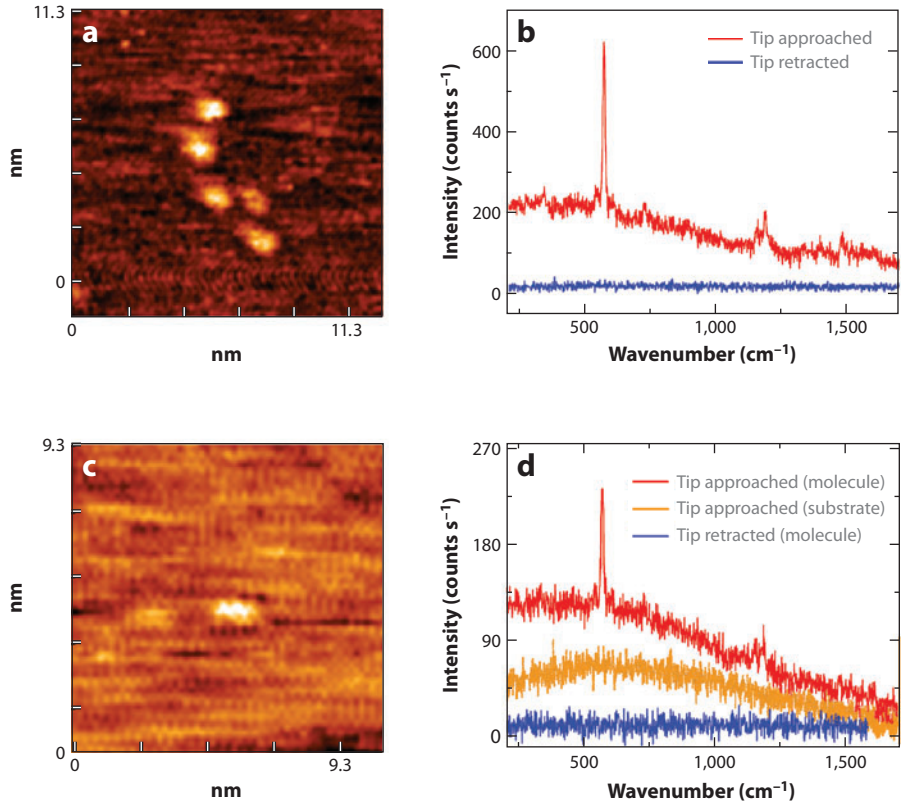

Figure 9

Scanning tunneling microscope images of five BCB molecules (*a*) and a single BCB molecule (*c*) adsorbed on Au(111), and the resonance Raman and TER spectra (*b*,*d*). The spectra were recorded with an integration time of 1 s; all measurements occurred under ultrahigh vacuum conditions. Adapted with permission from Reference 12. Copyright 2008 The American Physical Society.

contributed approximately 87 cps to the total signal. For the experiments described in (12), the coverage of BCB was so small that STM images of surface sections of approximately 12×12 nm^2 showed only a few, or even a single, BCB molecule; the molecules seem to be fixed on defect sites. For the tip centered over the molecular group or over the single molecule, the TER intensities amounted to 410 cps for five BCB molecules, and to approximately 90 cps for a single BCB molecule. In the latter case, the spectra reveal an S/N of $90/20 > 4$. Thus, STM images and the TER spectrum indicate remarkable evidence for single-molecule TERS.

The advantages of the UHV-TERS approach are manifold: (*a*) monitoring and control of adsorption, (*b*) high surface quality, (*c*) minimization of impurities, (*d*) SPM imaging of small sections of surfaces covered with either a monolayer or a submonolayer of adsorbates, or even with well-separated, individual molecules, (*e*) significantly lower photodegradation of adsorbed molecules under UHV conditions.

The experiment discussed below highlights these UHV-TERS advantages. Here, advantage is taken of a preparation chamber added to the UHV-TERS system. It permits the sputtering and annealing of the substrates as well as the evaporation of molecules. Again, Au(111) surfaces were used as substrates. The UHV-based preparation of the sample leads to atomically smooth Au(111), and STM images show large (111)-oriented, monoatomic terraces and three domains of the Herringbone reconstruction, indicating the smoothness of the sample and minimal impurities.

Fullerene C_{60} molecules were chosen as adsorbates and were evaporated in low doses onto the smooth Au(111) surface. STM images reveal that the deposited C_{60} molecules form small islands of approximately 40-nm diameter, preferentially aligned along monoatomic steps; whereas, the major part of the surface is free of C_{60} and still exhibits the characteristic Herringbone reconstruction. In **Figure 10**, the inset exhibits a 15.5×15.5 nm^2 region of such an island, where the C_{60} molecules assume a hexagonal structure (84).

Most interesting are the TER spectra of such islands: A small island contains roughly 1,200 C_{60} molecules; for a sharp tip ($R_{tip} \sim 20$nm), the TERS region (i.e., the region of the enhanced field zone) has a diameter of ~20 nm; therefore, within this region, only 300 C_{60} molecules are present and only these contribute to TERS. After retraction of the tip, no Raman signal can be detected. **Figure 10** shows TER spectra from a C_{60} island. Because of the low incident laser power used ($P_L = 0.1$ mW) and the short acquisition time (0.5 s), the TER signal is relatively low, and consequently, the spectral curves show substantial noise. However, as a spectrum is recorded every 0.5 s over a time interval of more than 50 s in this experiment, over 100 spectra are available for analysis. Instead of simple smoothing, eight groups of 16 successive spectra were averaged, where for each group the starting spectrum number is increased by ten; i.e., the first average spectrum covers the time range from the 0th second to the 8th second; the second average spectrum, from the 5th second to the 13th second; and so on. Although this procedure reduces the noise, it also averages away possible short time dependencies of the individual Raman bands, at least to some extent. Nevertheless, over the whole time period, each average spectrum deviates from the previous one in characteristic ways: The intensity drops in general; the relative intensities alter significantly; and frequencies shift to some extent. Nonetheless, all the individual >100 spectra and their various averages taken from this set of spectra display the general pattern of C_{60} TERS.

The above described spectral variations indicate that remarkable changes within the C_{60} island occur during TERS measurements. Indeed, STM images before and after TERS measurement show the same island, but with altered composition. Possible causes are increased diffusion induced by the tip, which is common at room temperature; structural changes may also be caused by the enhanced incident field, photodesorption, photochemistry, or even photodegradation of the molecules. Connected with this are changes in the local adsorption sites and lateral interactions between the C_{60} molecules, and all this may lead to the observed spectral variations in TERS.

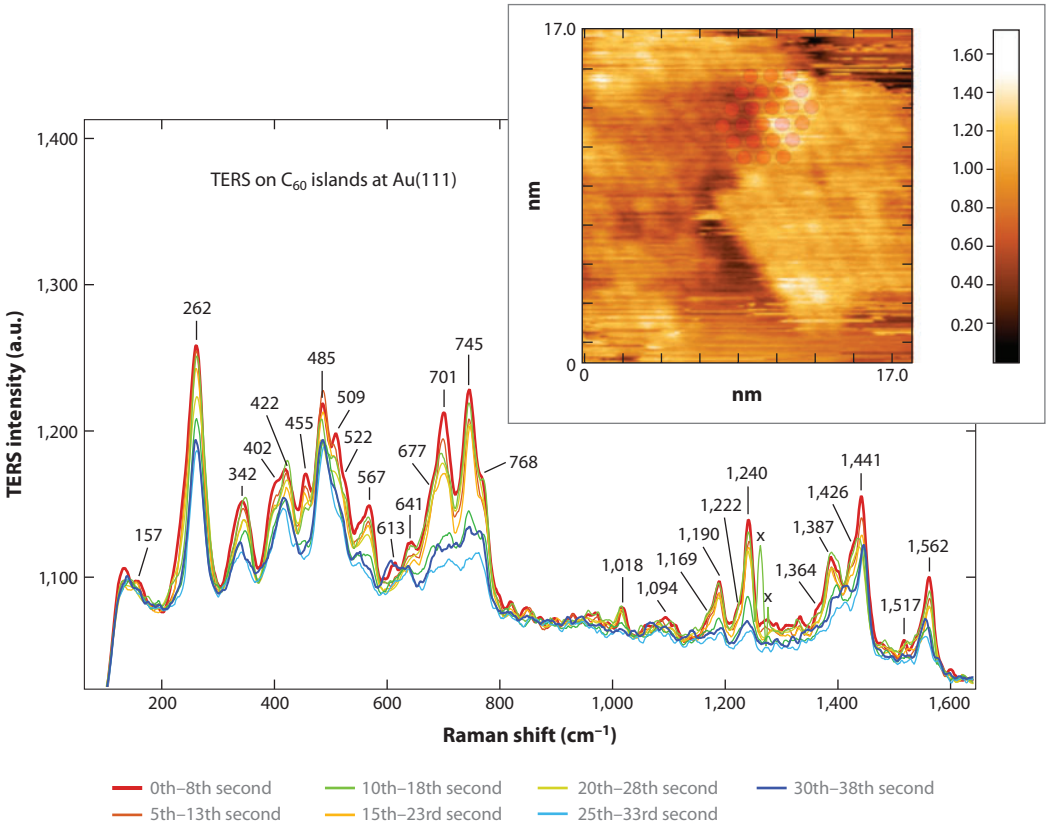

Figure 10

Tip-enhanced Raman spectra on a C_{60} island at Au(111). The spectra are subsequently recorded every 0.5 s and grouped into eight sets of averaged spectra (each over 16 original spectra) with a time delay for each group from the former of 5 s. Incident laser power is 0.1 mW. $\lambda_{ex} = 632.8$ nm. The color code for the eight spectra indicates time dependence. (*Inset*) Scanning tunneling microscope image of a C_{60} island on a Au(111) surface across a monoatomic Au step. A scheme of (111)-oriented C_{60} molecules is overlayed in the top region of the image analogous to Tang et al. (80, figure 7b). Abbreviation: TERS, tip-enhanced Raman spectroscopy.

In 2010, Luo et al. (81) published a paper concerning single-molecule SERS (SM-SERS) for C_{60} fullerenes at Au nanoparticles. The authors observed spectral variations for distinct hot spots as well as spectral fluctuations with time and ascribed these effects to the single-molecule behavior; whereas, the appearance of new bands and band splitting were attributed to the symmetry reduction of C_{60} upon adsorption. TERS measurements on C_{60} islands, described here, show spectral patterns that closely resemble the SM-SERS spectra reported by Luo et al. (81).

Table 1 illustrates these findings, comparing data from Luo et al. (81) (columns 1–3) and data from Ikeda & Uosaki (83) (column 5), with UHV-TERS data (columns 6 and 7) and with frequencies and symmetry assignment from Menéndez & Page (82, table 2.4) (columns 8 and 9). Columns 1–3 look at SM-SERS on three different hot spots [note that our tip-C_{60}/Au(111) configuration (data are shown in column 7, whereas column 6 indicate whether a peak or a shoulder is observed) essentially represents a single hot spot]. Column 4 is the symmetry assignment given by Luo et al. Note that there are some discrepancies in the assignment, which will not be discussed

Table 1 Raman shifts for an island of fullerene C_{60} molecules deposited on a Au(111) surface

SM-SERS of C_{60} at different hot spots[a]				Resonant Raman at 785 nm[b]	UHV-TERS at C_{60} islands, 633 nm[c,e]		Frequencies of isolated C_{60} molecules[d]	
785 nm[a]			Symmetry[a]					Symmetry[d,f]
1	2	3	4	5	6	7	8	9
254	268	273	$H_g(1)$	271	**p**	**262**	272	$H_g(1)$
269	309	308						
344	341	347	$T_{2u}(1)$		**p**	**342**	342	$T_{3u}(1)$
							358	$G_u(1)$
381		388			**s**	**402**	403	$H_u(1)$
400	402		$H_g(2)$	432	**p**	**422**	433	$H_g(2)$
425	425	433						
					p	**485**	485	$G_g(1)$
491	492	495	$A_g(1)$	495	**p**	**509**	496	$A_g(1)$
517	521		$T_{1u}(1)$		s	524	526	$T_{1u}(1)$
							534	$H_u(2)$
					s	554	553	$T_{3g}(1)$
							567	$G_g(2)$
544	565	561	$T_{1u}(2)$				568	$T_{1g}(1)$
					p	**567**	575	$T_{1u}(2)$
612	597	602				613		
633		620						
	647					641		
659		661	$H_g(3)$		s	**677**	668	$H_u(3)$
686	678							
704	704	707		709	**p**	**701**	709	$H_g(3)$
	734	748			**p**	**745**	736	$G_g(3)$
							743	$H_u(4)$
770	770		$H_g(4)$	770	s	**768**	772	$H_g(4)$
	797	784					796	$T_{3g}(3)$
825	832	827	G_o				831	$T_{1g}(2)$
870	875							
886		888						
934	929	932	$T_{1g}(1)$					
961	961		$T_{2u}(1)$			957	961	$G_u(4)$
981		985					984	A_u
	999							
1,031	1,026	1,032			**p**	**1,018**		
1,071		1,081	$H_g(5)$				1,079	$G_g(4)$
1,093	1,100	1,116		1,097	**p**	**1,094**	1,099	$H_g(5)$
1,136	1,147							
					s	1,169		
1,180	1,187	1,160	G_g					
1,209		1,196	$T_{1u}(3)$		**p**	**1,190**	1,182	$T_{1u}(3)$
							1,205	$T_{3u}(4)$

(*Continued*)

Table 1 (*Continued*)

SM-SERS of C_{60} at different hot spots[a]				Resonant Raman at 785 nm[b]	UHV-TERS at C_{60} islands, 633 nm[c,e]		Frequencies of isolated C_{60} molecules[d]	
785 nm[a]			Symmetry[a]					Symmetry[d,f]
1	2	3	4	5	6	7	8	9
1,223		1,229	$H_g(6)$		s	1,222	1,223	$H_u(5)$
1,244				1,250	**p**	1,240	1,252	$H_g(6)$
1,269	1,269	1,264						
1,289		1,292					1,289	$T_{1g}(3)$
1,319		1,332						
	1,344		T_{1g}			1,332	1,344	$H_u(6)$
					s	1,364		
		1,386			**p**	**1,387**		
1,419	1,428	1,430	$H_g(7)$	1,426	**s**	**1,426**	1,425	$H_g(7)$,
1,419	1,428	1,430	$T_{1u}(4)$		**s**	**1,426**	1,429	$T_{1u}(4)$
1,464	1,462		$A_g(2)$	1,468	**p**	**1,441**	1,470	$A_g(2)$
1,497	1,498						1,482	$G_g(6)$
						1,517	1,525	$T_{3u}(5)$
1,538	1,564	1,552	$H_g(8)$		s	1,543	1,567	$H_u(7)$
1,585	1,604	1,582		1,574	**p**	**1,562**	1,575	$H_g(8)$

[a]Data adapted with permission from Reference 81. Copyright (2010) Wiley & Sons Ltd.
[b]Data adapted with permission from Reference 83. Copyright (2008) American Chemical Society.
[c]Data from this work.
[d]Data taken with kind permission from Reference 82. Copyright (2000) Springer Science+Business Media.
[e]Bold and nonbold items indicate clearly visible and very weak bands or shoulders, respectively.
[f]The ten Raman active modes are indicated by eight light-green (H_g symmetry) and two light-blue (A_g symmetry) rows; the four infrared active modes (T_{1u} symmetry) are indicated by four light-red rows. Assignment in the first through fifth column is according to Reference 81. Assignment in the sixth through ninth column is according to Reference 82.
Abbreviations: p, peak; s, shoulder; SM-SERS, single-molecule–surface-enhanced Raman spectroscopy; UHV-TERS, ultrahigh vacuum–tip-enhanced Raman spectroscopy.

here. Column 5 shows the ten allowed Raman frequencies for a C_{60} film observed with a 785-nm exciting line, reported by Ikeda & Uosaki (83). The UHV-TERS data (column 7) are taken with the 633-nm line of a helium-neon laser, using 0.1 mW incident power (84). Most bands differ in frequency by only a few wavenumbers from the results of Luo et al. as well as from Menéndez et al. Thus, for the assignment, we make use of the data of Menéndez et al., which are only strictly valid for isolated C_{60} molecules having I_h symmetry. For better readability, colors are added to 14 rows assigned either with H_g symmetry (8 green rows), A_g symmetry (2 blue rows), or with T_{1u} (4 light-red rows) indicating ten Raman active and 4 infrared active modes, respectively; the fact that more than 30 vibrational modes are seen in TERS of C_{60} molecules indicates a significant reduction in symmetry due to the adsorption and formation of C_{60} islands at an Au(111) surface. A detailed discussion of the spectral assignments and the influence of symmetry reduction (by adsorption and/or by formation of a two-dimensional hexagonal structure) is beyond the scope of this review. Further UHV-TER experiments on freshly prepared C_{60} islands also yielded remarkable spectral fluctuations in time, showing slightly different spectral patterns. These experiments indicate a remarkable variability of C_{60} islands in structure, adsorption, and lateral interactions (84).

Often, spectral fluctuations, similar to those obtained with UHV-TERS or even more severe, have been considered as the proof for single-molecule SERS or single-molecule TERS, whereas ensemble-averaged SERS or TERS is believed to show no spectral fluctuations. The above described experiment provides additional information: STM images from the investigated region showing hundreds of relatively ordered C_{60} molecules in an island. Yet, such an ensemble of molecules also shows significant spectral fluctuations. These observations rule out the idea that spectral fluctuations necessarily point to single-molecule events. Without doubt, these preliminary results require further detailed investigation into the causes of the observed spectral variation. Corresponding experiments are on the way.

4. CONCLUSION

TERS overcomes most of the drawbacks of SERS but keeps its advantages, such as its high sensitivity. In addition, TERS provides a very high spatial resolution, much beyond the Abbe limit. TERS permits the correlation of topographic and chemical data, finding application in a number of fields, such as surface science, material science, and biology. Single-molecule TERS has been observed even for TER enhancements of "only" 10^6 to 10^7. A condensed overview concerning measured contrasts and estimated total enhancements and a discussion reveal that an extreme enhancement $\gg 10^7$ in combination with a high laser power is probably counterproductive as its associated local intensity may affect or even destroy adsorbed molecules. Finally, preliminary results of UHV-TERS on a C_{60} island were presented; these islands have a diameter of a few tens of nanometers and are deposited on a smooth Au(111) surface. Most striking is TERS' significant time dependence for C_{60}, not so much in frequencies but in general intensity and in relative band intensities as this can point to structural, adsorptive, and chemical changes within the C_{60} adlayer. The remarkable variability of C_{60} TER spectra makes this system an interesting laboratory for molecule-substrate and intermolecular interactions.

SUMMARY POINTS

1. SERS focuses on the concept of a few hot spots that make the most of the signal and that in a sense led to TERS.
2. TERS is based on a single hot spot, a narrow gap between the tip and sample, but avoids the drawbacks of SERS.
3. The presentation of some early TERS experiments shows TERS for a variety of systems and large variations in contrast and underlying enhancement.
4. A comparison of contrast and overall enhancement data for TERS based on AFM, shear force, and STM reveals large differences in measured contrast as well as in the estimation of underlying enhancements.
5. A moderate enhancement of "only" $\sim 10^6$ is sufficient to achieve few-molecule TERS. Significantly higher enhancements may cause photodegradation.
6. UHV-TERS combines the advantages of a UHV system with those of TERS. Vibrational spectroscopy studies on a single or a few molecules on otherwise clean surfaces become achievable. This high sensitivity of TERS may lead to its application in the field of heterogeneous catalysis.

DISCLOSURE STATEMENT

The authors are not aware of any affiliations, memberships, funding, or financial holdings that might be perceived as affecting the objectivity of this review.

ACKNOWLEDGMENTS

The authors gratefully acknowledge Prof. M. Wolf for his scientific advice and generous support of this UHV-TERS project and Prof. H.J. Freund for his very valuable support as our host. The authors also gratefully acknowledge W. Mahdi for carefully reading the manuscript and S. Kubala, D. Bauer, S. Hagen, and K.P. Vogelsang for their substantial help in upgrading the UHV-TERS system.

LITERATURE CITED

1. **Stockle RM, Suh YD, Deckert V, Zenobi R. 2000. Nanoscale chemical analysis by tip-enhanced Raman spectroscopy. *Chem. Phys. Lett.* 318:131–36**
2. Anderson MS. 2000. Locally enhanced Raman spectroscopy with an atomic force microscope. *Appl. Phys. Lett.* 76:3130–32
3. Hayazawa N, Inouye Y, Sekkat Z, Kawata S. 2000. Metallized tip amplification of near-field Raman scattering. *Opt. Commun.* 183:333–36
4. Pettinger B, Picardi G, Schuster R, Ertl G. 2000. Surface enhanced Raman spectroscopy: towards single molecular spectroscopy. *Electrochemistry (Jpn.)* 68:942–49
5. Chang RK, Furtak TE, eds. 1982. *Surface-Enhanced Raman Spectroscopy*. New York: Plenum
6. Tian ZQ, Ren B, Mao BW. 1997. Extending surface Raman spectroscopy to transition metal surfaces for practical applications. 1. Vibrational properties of thiocyanate and carbon monoxide adsorbed on electrochemically activated platinum surfaces. *J. Phys. Chem. B* 101:1338–46
7. Pettinger B, Picardi G, Schuster R, Ertl G. 2003. Surface-enhanced and STM tip-enhanced Raman spectroscopy of CN^- ions at gold surfaces. *J. Electroanal. Chem.* 554:293–99
8. Pettinger B, Picardi G, Schuster R, Ertl G. 2004. Nanoscale probing of adsorbed species by tip-enhanced Raman spectroscopy. *Phys. Rev. Lett.* 92:96101
9. Mehtani D, Lee N, Hartschuh RD, Kisliuk A, Foster MD, et al. 2005. Nano-Raman spectroscopy with side-illumination optics. *J. Raman Spectrosc.* 36:1068–75
10. **Steidtner J, Pettinger B. 2007. High-resolution microscope for tip-enhanced optical processes in ultrahigh vacuum. *Rev. Sci. Instrum.* 78:103104**
11. Domke KF, Zhang D, Pettinger B. 2007. Tip-enhanced Raman spectra of picomole quantities of DNA nucleobases at Au(111). *J. Am. Chem. Soc.* 129:6708–9
12. Steidtner J, Pettinger B. 2008. Tip-enhanced Raman spectroscopy and microscopy on single dye molecules with 15 nm resolution. *Phys. Rev. Lett.* 100:236101
13. **Jeanmaire DL, Van Duyne RP. 1977. Surface Raman spectroelectrochemistry. 1. Heterocyclic, aromatic, and aliphatic-amines adsorbed on the anodized silver electrode. *J. Electroanal. Chem.* 84:1–20**
14. **McQuillan AJ, Hendra PJ, Fleischmann M. 1975. Raman spectroscopic investigation of silver electrodes. *J. Electroanal. Chem.* 65:933–44**
15. Fleischmann M, Hendra PJ, McQuillan AJ, Pual RL, Reid ES. 1976. Raman-spectroscopy at electrode-electrolyte interfaces. *J. Raman Spectrosc.* 4:269–74
16. King FW, Van Duyne RP, Schatz GC. 1978. Theory of Raman scattering by molecules adsorbed on electrode surfaces. *J. Chem. Phys.* 69:4472–81
17. Otto A. 1980. Surface enhanced Raman-scattering (SERS): What do we know? *Appl. Surf. Sci.* 6:309–55
18. Ueba H, Ichimura S, Yamada H. 1982. Where are we in the study of SERS? Role of chemisorption and charge transfer. *Surf. Sci.* 119:433–48

1. First report on tip-enhanced Raman spectroscopy (TERS).

10. First TERS under UHV conditions.

13. First recognition of a surface-enhanced Raman effect.

14. First Raman experiment on silver electrodes.

19. Pettenkofer C, Pockrand I, Otto A. 1983. Surface enhanced Raman spectra of oxygen adsorbed on silver. *Surf. Sci.* 135:52–64
20. Adrian F. 1983. Charge-transfer effects in surface enhanced Raman scattering. *J. Electron. Spectrosc.* 29:349
21. Shalaev VM, Stockmann MI. 1988. Fractals: optical susceptibility and giant Raman scattering. *Z. Phys. D* 10:71–79
22. Shalaev VM, Sarychev AK. 1998. Nonlinear optics of random metal-dielectric films. *Phys. Rev. B* 57:13265–88
23. Kim W, Safonov VP, Shalaev VM, Armstrong RL. 1999. Fractals in microcavities: giant coupled, multiplicative enhancement of optical responses. *Phys. Rev. Lett.* 82:4811–14
24. Gresillon S, Aigouy L, Boccara AC, Rivoal JC, Quelin X, et al. 1999. Experimental observation of localized optical excitations in random metal-dielectric films. *Phys. Rev. Lett.* 82:4520–23
25. Gresillon S, Rivoal JC, Gadenne P, Quelin X, Shalaev VM, Sarychev A. 1999. Nanoscale observation of enhanced electromagnetic field. *Phys. Status Solidi A* 175:337–43
26. Markel VA, Shalaev VM, Zhang P, Huynh W, Tay L, et al. 1999. Near-field optical spectroscopy of individual surface-plasmon modes in colloid clusters. *Phys. Rev. B* 59:10903–9
27. Moskovits M. 2005. Surface-enhanced Raman spectroscopy: a brief retrospective. *J. Raman Spectrosc.* 36:485–96
28. Xu HX, Aizpurua J, Kall M, Apell P. 2000. Electromagnetic contributions to single-molecule sensitivity in surface-enhanced Raman scattering. *Phys. Rev. E* 62:4318–24
29. Xu HX, Kall M. 2002. Surface-plasmon-enhanced optical forces in silver nanoaggregates. *Phys. Rev. Lett.* 89:246802
30. Johansson P, Xu HX, Kall M. 2005. Surface-enhanced Raman scattering and fluorescence near metal nanoparticles. *Phys. Rev. B* 72:35427
31. Kall M, Xu HX, Johansson P. 2005. Field enhancement and molecular response in surface-enhanced Raman scattering and fluorescence spectroscopy. *J. Raman Spectrosc.* 36:510–14
32. Kneipp K, Wang Y, Dasari RR, Feld MS. 1995. Approach to single-molecule detection using surface-enhanced resonance Raman-scattering (SERRS)—a study using rhodamine 6g on colloidal silver. *Appl. Spectrosc.* 49:780–84
33. Kneipp K, Wang Y, Kneipp H, Perelman LT, Itzkan I, et al. 1997. Single molecule detection using surface-enhanced Raman scattering (SERS). *Phys. Rev. Lett.* 78:1667–70
34. Nie SM, Emory SR. 1997. Probing single molecules and single nanoparticles by surface-enhanced Raman scattering. *Science* 275:1102–6
35. Krug JT, Wang GD, Emory SR, Nie SM. 1999. Efficient Raman enhancement and intermittent light emission observed in single gold nanocrystals. *J. Am. Chem. Soc.* 121:9208–14
36. Etchegoin PG, Lacharmoise PD, Le Ru EC. 2009. Influence of photostability on single-molecule surface enhanced Raman scattering enhancement factors. *Anal. Chem.* 81:682–88
37. Pettinger B. 2010. Single-molecule surface- and tip-enhanced Raman spectroscopy. *Mol. Phys.* 108:2039–59
38. Yonzon CR, Stuart DA, Zhang XY, McFarland AD, Haynes CL, Van Duyne RP. 2005. Towards advanced chemical and biological nanosensors—an overview. *Talanta* 67:438–48
39. Stewart ME, Anderton CR, Thompson LB, Maria J, Gray SK, et al. 2008. Nanostructured plasmonic sensors. *Chem. Rev.* 108:494–521
40. Strelau KK, Schueler T, Moeller R, Fritzsche W, Popp J. 2010. Novel bottom-up SERS substrates for quantitative and parallelized analytics. *ChemPhysChem* 11:394–98
41. Campion A, Brown JK, Grizzle VM. 1982. Surface Raman-spectroscopy without enhancement—nitrobenzene on Ni(111). *Surf. Sci.* 115:L153–58
42. Harradine D, Campion A. 1987. Surface Raman-spectroscopy without enhancement—pyridine adsorbed on Ni(111) and Ni(100). *Chem. Phys. Lett.* 135:501–5
43. Campion A, Ivaecky JE, Child CM, Foster M. 1995. On the mechanism of chemical enhancement in surface-enhanced Raman scattering. *J. Am. Chem. Soc.* 117:11807–8
44. Kambhampati P, Child CM, Campion A. 1996. On the role of charge-transfer resonances in the chemical mechanism of surface-enhanced Raman scattering. *J. Chem. Soc. Faraday Trans.* 92:4775–80

22. First hot-spot concept for giant SERS.

36. Limitation of SERS enhancement factor to $<10^{11}$.

45. Kambhampati P, Campion A. 1999. Surface enhanced Raman scattering as a probe of adsorbate-substrate charge-transfer excitations. *Surf. Sci.* 428:115–25
46. Aravind PK, Metiu H. 1982. Use of a perfectly conducting sphere to excite the plasmon of a flat surface. 1. Calculation of the local field with applications to surface-enhanced spectroscopy. *J. Phys. Chem.* 86:5076–84
47. Aravind PK, Rendell RW, Metiu H. 1982. A new geometry for field enhancement in surface-enhanced spectroscopy. *Chem. Phys. Lett.* 85:396–403
48. Aravind PK, Metiu H. 1983. The effects of the interaction between resonances in the electromagnetic response of a sphere-plane structure—applications to surface enhanced spectroscopy. *Surf. Sci.* 124:506–28
49. Metiu H, Das P. 1984. The electromagnetic theory of surface enhanced spectroscopy. *Annu. Rev. Phys. Chem.* 35:507–36

50. First concept for TERS.

50. Wessel J. 1985. Surface-enhanced optical microscopy. *J. Opt. Soc. Am. B* 2:1538–41

51. Rasmussen A, Deckert V. 2006. Surface- and tip-enhanced Raman scattering of DNA components. *J. Raman Spectrosc.* 37:311–17
52. Neugebauer U, Schmid U, Baumann K, Ziebuhr W, Kozitskaya S, et al. 2007. Towards a detailed understanding of bacterial metabolism—spectroscopic characterization of *Staphylococcus epidermidis*. *ChemPhysChem* 8:124–37
53. Budich C, Neugebauer U, Popp J, Deckert V. 2008. Cell wall investigations utilizing tip-enhanced Raman scattering. *J. Microsc. Oxf.* 229:533–39
54. Harz A, Roesch P, Popp J. 2009. Vibrational spectroscopy—a powerful tool for the rapid identification of microbial cells at the single-cell level. *Cytom. Part A* 75A:104–13
55. Boehme R, Cialla D, Richter M, Roesch P, Popp J, Deckert V. 2010. Biochemical imaging below the diffraction limit—probing cellular membrane related structures by tip-enhanced Raman spectroscopy (TERS). *J. Biophotonics* 3:455–61
56. Wood BR, Bailo E, Khiavi MA, Tilley L, Deed S, et al. 2011. Tip-enhanced Raman scattering (TERS) from hemozoin crystals within a sectioned erythrocyte. *Nano Lett.* 11:1868–73
57. Pettinger B, Domke KF, Zhang D, Schuster R, Ertl G. 2007. Direct monitoring of plasmon resonances in a tip-surface gap of varying width. *Phys. Rev. B* 76:113409
58. Stanciu C, Sackrow M, Meixner AJ. 2008. High NA particle- and tip-enhanced nanoscale Raman spectroscopy with a parabolic-mirror microscope. *J. Microsc. Oxf.* 229:247–53
59. Saito Y, Motohashi M, Hayazawa N, Kawata S. 2008. Stress imagining of semiconductor surface by tip-enhanced Raman spectroscopy. *J. Microsc. Oxf.* 229:217–22
60. Yeo B-S, Stadler J, Schmid T, Zenobi R, Zhang W. 2009. Tip-enhanced Raman spectroscopy—its status, challenges and future directions. *Chem. Phys. Lett.* 472:1–13
61. Zhuang M, Liu Z, Ren B, Tian Z. 2010. Surface bonding on silicon surfaces as probed by tip-enhanced Raman spectroscopy. *Sci. China Chem.* 53:426–31
62. Zhang D, Domke KF, Pettinger B. 2010. Tip-enhanced Raman spectroscopic studies of the hydrogen bonding between adenine and thymine adsorbed on Au(111). *ChemPhysChem* 11:1662–65
63. Chaigneau M, Picardi G, Ossikovski R. 2010. Tip-enhanced Raman spectroscopy evidence for amorphous carbon contamination on gold surfaces. *Surf. Sci.* 604:701–5
64. Hennemann LE, Meixner AJ, Zhang D. 2010. Surface- and tip-enhanced Raman spectroscopy of DNA. *Spectrosc. Int. J.* 24:119–24
65. Georgi C, Hartschuh A. 2010. Tip-enhanced Raman spectroscopic imaging of localized defects in carbon nanotubes. *Appl. Phys. Lett.* 97:143117
66. Pettinger B, Ren B, Picardi G, Schuster R, Ertl G. 2005. Tip-enhanced Raman spectroscopy (TERS) of malachite green isothiocyanate at Au(111): bleaching behavior under the influence of high electromagnetic fields. *J. Raman Spectrosc.* 36:541–50
67. Hayazawa N, Inouye Y, Sekkat Z, Kawata S. 2002. Near-field Raman imaging of organic molecules by an apertureless metallic probe scanning optical microscope. *J. Chem. Phys.* 117:1296–301
68. Hayazawa N, Tarun A, Inouye Y, Kawata S. 2002. Near-field enhanced Raman spectroscopy using side illumination optics. *J. Appl. Phys.* 92:6983–86
69. Pettinger B, Picardi G, Schuster R, Ertl G. 2002. Surface-enhanced and STM-tip-enhanced Raman spectroscopy at metal surfaces. *Single Mol.* 3:285–94

70. Hayazawa N, Yano T, Watanabe H, Inouye Y, Kawata S. 2003. Detection of an individual single-wall carbon nanotube by tip-enhanced near-field Raman spectroscopy. *Chem. Phys. Lett.* 376:174–80
71. Bulgarevich D, Futamata M. 2004. Apertureless tip-enhanced Raman microscopy with confocal epi-illumination/collection optics. *Appl. Spectrosc.* 58:757–61
72. Ren B, Picardi G, Pettinger B. 2004. Preparation of gold tips suitable for tip-enhanced Raman spectroscopy and light emission by electrochemical etching. *Rev. Sci. Instrum.* 84:837–41
73. Yeo B-S, Schmid T, Zhang W, Zenobi R. 2007. Towards rapid nanoscale chemical analysis using tip-enhanced Raman spectroscopy with Ag-coated dielectric tips. *Anal. Bioanal. Chem.* 387:2655–62
74. Vannier C, Yeo B, Melanson J, Zenobi R. 2006. Multifunctional microscope for far-field and tip-enhanced Raman spectroscopy. *Rev. Sci. Instrum.* 77:023104
75. Neugebauer U, Roesch P, Schmitt M, Popp J, Julien C, et al. 2006. On the way to nanometer-sized information of the bacterial surface by tip-enhanced Raman spectroscopy. *ChemPhysChem* 7:1428–30
76. Domke KF, Zhang D, Pettinger B. 2006. Toward Raman fingerprints of single dye molecules at atomically smooth Au(111). *J. Am. Chem. Soc.* 128:14721–27
77. Zhang W, Yeo BS, Schmid T, Zenobi R. 2007. Single molecule tip-enhanced Raman spectroscopy with silver tips. *J. Phys. Chem. C* 111:1733–38
78. Stadler J, Schmid T, Zenobi R. 2010. Nanoscale chemical imaging using top-illumination tip-enhanced Raman spectroscopy. *Nano Lett.* 10:4514–20
79. Chaigneau M, Picardi G, Ossikovski R. 2011. Molecular arrangement in self-assembled azobenzene-containing thiol monolayers at the individual domain level studied through polarized near-field Raman spectroscopy. *Int. J. Mol. Sci.* 12:1245–58
80. Tang L, Zhang X, Guo Q. 2010. Organizing C_{60} molecules on a nanostructured Au(111) surface. *Surf. Sci.* 604:1310–14
81. Luo Z, Loo BH, Peng A, Ma Y, Fu HB, Yao Y. 2010. Single molecule surface-enhanced Raman scattering of fullerene C_{60}. *J. Raman Spectrosc.* 42:319–23
82. Menéndez J, Page JB. 2000. Vibrational spectroscopy of C^{60}. *Top. Appl. Phys.* 76:27–95
83. Ikeda K, Uosaki K. 2008. Resonance hyper-Raman scattering of fullerene C_{60} microcrystals. *J. Phys. Chem. A* 112: 790–93
84. Schambach P, Villagomez CJ, Scott N, Wolf M, Pettinger B. 2012. Tip-enhanced Raman spectroscopy on C_{60} islands at Au(111) in UHV. Manuscript in preparation

Annual Review of
Physical Chemistry
Volume 63, 2012

Contents

Indexes

Errata

An online log of corrections to Annual Review of Physical Chemistry chapters (if any, 1997 to the present) may be found at http://physchem.AnnualReviews.org/errata.shtml